American Journal of Medical Genetics 113:144–150 (2002)

Delimitation of Duplicated Segments and Identification of Their Parental Origin in Two Partial Chromosome 3p Duplications

Sylvie Antonini,[1] Chong A. Kim,[2] Sofia M. Sugayama,[2] and Angela M. Vianna-Morgante[1]*
[1]*Departamento de Biologia, Instituto de Biociências, Universidade de São Paulo, Brazil*
[2]*Instituto da Criança, Universidade de São Paulo, São Paulo, Brazil*

Two chromosome 3 short arm duplications identified through G-banding were further investigated using fluorescence in situ hybridization (FISH) and polymerase chain reaction (PCR) of microsatellite markers, aiming at mapping breakpoints and disclosing mechanisms of origin of these chromosome aberrations. Patient 1 was found to be a mosaic: a 3p12 → 3p21 duplication was observed in most of his cells, and a normal cell line occurred with a frequency of about 3% in blood. In situ hybridization of chromosome 3 short- and long-arm libraries confirmed the short-arm duplication. Using FISH of short-arm sequences, the YAC 961_h_3 was shown to contain the proximal breakpoint (3p12.1 or 3p12.2), and the distal breakpoint was located between the YACs 729_c_3 and 806_h_2, which are adjacent in the WC 3.10 contig (3p21.1). In Patient 2, G-banding indicated a 3p21 → 3p24 duplication, without mosaicism. In situ hybridization of chromosome 3 short- and long-arm libraries confirmed the duplication of short-arm sequences. FISH of chromosome 3 sequences showed that the YAC 749_a_7 spanned the proximal breakpoint (3p21.33). The distal breakpoint mapped to the interval between YACs 932_b_6 (3p24.3) and 909_b_6 (3p25). In both cases, microsatellite genotyping pointed to a rearrangement between paternal sister chromatids. © 2002 Wiley-Liss, Inc.

KEY WORDS: chromosomal duplication; chromosome 3; mental retardation/multiple congenital anomalies (MR/MCA) syndrome

INTRODUCTION

Chromosomal abnormalities are one of the major causes of mental retardation/multiple congenital anomalies syndromes. The precise identification of duplicated/deleted chromosomal segments and of their parental origin is requisite for delineating the clinical consequences of these unbalances. The availability of cloned segments covering the human chromosomes as probes for fluorescence in situ hybridization (FISH) allowed a much more precise delimitation of the altered segments and breakpoint mapping than had been possible based on banding patterns [Floridia et al., 1996; Page et al., 1996; Huang et al., 1997; Wandstrat et al., 1998; Christ et al., 1999]. When the analysis of DNA polymorphisms is associated, it not only adds to the precision of this mapping, but also constitutes a tool for disclosing parental origin of the chromosomal abnormality [Katz et al., 1999; Giglio et al., 2000; Rosenberg et al., 2000]. Parent-of-origin determination becomes important in these studies since, as a consequence of genome imprinting, it is a potential additional cause of the clinical variability of chromosomal unbalances [Sutton and Shaffer, 2000]. Eventually, this analysis also contributes to disclosing the mechanisms leading to chromosomal abnormalities [Floridia et al., 1996; Lupski, 1998; Katz et al., 1999; Giglio et al., 2000].

In the two partial short-arm duplications of chromosome 3 herein described, we delimited the duplicated segments and mapped the breakpoints, using both FISH and microsatellite genotyping by PCR. The most likely mechanisms that led to the formation of these chromosomal aberrations could be inferred.

CLINICAL REPORTS

Patient 1 (RFM 23/10/80, Fig. 1a) was the first son of nonconsanguineous parents and had two normal sibs.

Grant sponsor: FAPESP and CNPq.

*Correspondence to: Angela M. Vianna-Morgante, Departamento de Biologia, Instituto de Biociências, Universidade de São Paulo, CP 11461, CEP 05422-970, São Paulo, SP, Brazil.
E-mail: avmorgan@ib.usp.br

Received 13 March 2001; Accepted 15 May 2002
DOI 10.1002/ajmg.10735

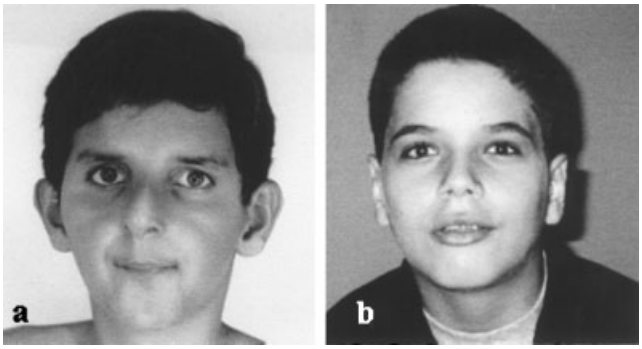

Fig. 1. **a:** Patient 1 at 13½ years of age. **b:** Patient 2 at 11 years of age.

He was born at term, by cesarean section, after an uncomplicated pregnancy. Birth weight was 3,360 g, length was 49 cm, and head circumference was 49 cm (all values in the normal range). Congenital bilateral clubfoot was surgically corrected. He walked at the age of 2 years and speech started at the age of 1½ years. He was first examined by us (C.A.K. and S.M.S.) at the age of 13½ years because of short stature, moderate mental retardation, and facial anomalies. At physical examination, his weight was 26 kg and height was 136 cm (both <3rd centile). Clinical features included narrow forehead, prominent glabella, low frontal hairline, deep-set eyes, beaked nose with prominent nasal bridge (right-turned nasal septum had been surgically corrected), long philtrum, high arched palate; protruding ears, the left ear being larger than the right one; long fingers with pads, muscular atrophy of lower limbs; scoliosis to the right and prominent lordosis. Radiographs of upper limbs and pelvis did not show abnormalities. Radiographs of the lower limbs revealed bone demineralization, bilateral varum deformity of fibula, and bilateral narrowing of the cortical portion of the tibia and fibula. Echocardiogram did not reveal abnormalities. At 17 years of age, his weight (38.2 kg) and height (154 cm) were still below the 3rd centile, but head circumference was in the normal range (54.5 cm).

Patient 2 (AAS 28/01/87, Fig. 1b) was the first son of nonconsanguineous parents. He was born at term by cesarean section and weighed 3,500 g. He presented with hypotonia. Motor milestones were delayed: he held his head up at 6 months of age, sat at the age of 1 year, and walked at 2½ years. At the age of 3 years, he could not speak in sentences. Sphincter control was achieved at that time. The patient was referred to us (C.A.K. and S.M.S.) at 7 years of age because of neuropsychomotor developmental delay associated with mild physical abnormalities. Weight was 28.5 kg (90th–97th centile), stature, 127 cm (75th–90th centile) and head circumference, 55 cm (>98th centile). Physical examination revealed wide forehead, anteverted nares, long and deep nasal philtrum, high arched palate, and large ears with hypoplastic cartilage. Digits were long and tapering, and partial syndactyly of second and third digits was observed. Mild bilateral genu valgum and flat feet were present. He had joint hyperextensibility and mild scoliosis, with the left scapula higher than the right one. A café-au-lait spot was present at the upper dorsum. At that time, he appeared mildly mentally retarded and presented abnormal behavior, with hyperactivity, repetitive hand biting and perseveration in speech. Radiography of the head, spine, long bones, and hands did not reveal abnormalities, but calcifications were revealed at the pelvis. A right temporal arachnoid cyst was detected by computed tomography scan. Ophthalmological examination did not show abnormalities. At 11 years, his height was 152 cm (90th–97th centile) and he presented macrocrania (occipital-frontal circumference = 57 cm, 98th centile).

METHODS

Cytogenetic Studies

Chromosomal analyses were performed on cultured peripheral blood lymphocytes, after GTG-banding and FISH.

FISH was performed in order to delimit the duplicated region. Probes included chromosome 3 short- and long-arm libraries that were hybridized according to the manufacturer (American Laboratory Supplies, Inc., Arlington, VA); plasmid pα3.5 containing chromosome 3 alphoid DNA sequences [Waye and Willard, 1989]; overlapping cosmids c64D1 and c81E4 that contain sequences from the *FHIT* gene (3p14.2), and overlapping cosmids c59H8 and c98A10, which contain sequences from the HSema IV gene (3p21.31), a gift from Dr. M. Garcia-Varella, University of Colorado Health Sciences Center; 25 YAC clones mapped to 3p and obtained from the CEPH YAC library. The hybridization was performed as previously described [Rosenberg et al., 1994], with minor modifications. Probes were labeled with biotin or digoxigenin by nick translation (Roche, Mannhein, Germany). The hybridization of α-satellite was carried out at 37°C overnight, and of cosmids and YACs, at 37°C for a week. The detection of probes was accomplished by incubation with fluorescein isothiocyanate (FITC) avidin (Vector, Burlingame, CA), or with rhodamine antidigoxigenin/FITC avidin (ONCOR, Gaithersburg, MD). Slides were mounted with Vectashield Mounting Medium (Vector) containing DAPI (4′,6-diamidino-2-phenyl-indole). At least 30 metaphases were analyzed in each experiment, under a Zeiss Axiophot fluorescence microscope. Metaphase images were captured with a CCD camera and processed using ISIS software (MetaSystem, Attlussheim, Germany).

Genomic DNA from peripheral white blood cells of patients and their parents was extracted with phenol by routine methods. The genotyping of 17 highly polymorphic microsatellite loci mapped to 3p was performed by PCR standard techniques. Primer sequences and amplification conditions were obtained from the Genome Database (http://gdbwww.gdb.org). Radioactively labeled [(α^{32}P) dATP] PCR products were separated by electrophoresis on denaturing polyacrylamide gels, followed by autoradiography. Quantitative analysis was performed to assess loci duplications. The optical density (OD) of bands in autoradiograms were estimated using BIORAD GS 700 Image Densitometer (BIORAD

Laboratories, Inc., Hercules, CA). The ratio ($R_{a1/a2}$) between OD of the smaller (a1) and larger (a2) alleles was calculated for each locus in patients, both parents of Patient 1, and the mother of Patient 2. The dosage coefficients were estimated by dividing the patient ratio [$(R_{a1/a2})_P$] by the ratio obtained for parents [$(R_{a1/a2})_F$ and $(R_{a1/a2})_M$]. Dosage coefficients ≥ 1.5 and ≤ 0.75 were considered as indicative of duplications of the smaller and the larger alleles, respectively

RESULTS

Patient 1

Cytogenetic analysis. In 146/150 metaphases analyzed, a tandem 3p12 → 3p21 duplication was observed; the remaining four metaphases had a normal 46,XY karyotype (Fig. 2a). Both parents had normal karyotypes. In situ hybridization of chromosome 3 short- and long-arm libraries confirmed a short-arm duplication (Fig. 3a). Centromeric sequences did not appear duplicated. The cosmids containing sequences of the gene *FHIT* (3p14.2) were duplicated but HSema IV cosmids (3p21.31) were not. FISH of a YAC panel mapping around the putative breakpoints allowed the identification of the duplicated and nonduplicated segments, and enabled us to narrow the breakpoint regions. At the proximal breakpoint, the YACs 796_c_4 and 773_b_3 were duplicated, but the YACs 722_b_8 and 955_b_8 were not. The YAC 961_h_3 (mapped to 3p21.1 or 3p21.2) was duplicated, but the distal signal was consistently weaker, indicating that this YAC was only partially duplicated and contained the proximal breakpoint (Fig. 3b). The YACs 773_b_3 and 955_b_8, which flank YAC 961_h_3 in the contig WC 3.13, were duplicated and nonduplicated, respectively, thus confirming the localization of the proximal breakpoint. The same strategy was followed for mapping the distal breakpoint. YACs 730_c_5, 737_e_4, 755_f_12, 710_f_11, 922_d_5, 679_c_12, and 729_c_3 were duplicated, but YACs 887_f_12, 958_f_12, and 806_h_2 were not. YACs 729_c_3 (duplicated, Fig. 3c) and 806_h_2 (nonduplicated, Fig. 3d), adjacent in the WC 3.10 contig, were the last nonduplicated and the first duplicated segments and, since YAC 729_c_3 yielded signals of similar intensities, the distal breakpoint could be located between these two YACs. Dual-color FISH confirmed that the duplication was in tandem (Fig. 3e). Figure 4a summarizes FISH findings in this patient.

Microsatellite analysis. Eight microsatellite loci mapped to the duplicated segment and to the nonduplicated distal 3p were genotyped in the patient and his parents (Fig. 5a and c). Two different alleles were always present in the patient (loci D3S1110, D3S2336, D3S1277, D3S1514, D3S1540, D3S1296, D3S1542), except for the most proximal locus, D3S1663, in which he was homozygous. Allele dosage was compared by densitometry in loci D3S1514 and D3S1540, mapped to the duplicated segment, and in loci D3S2336 and D3S1277, mapped to the nonduplicated distal 3p. In loci D3S1514 and D3S1540, the paternal allele was clearly more amplified, and in loci D3S2336 and D3S1277 no difference between the intensities of paternal and maternal alleles was detected.

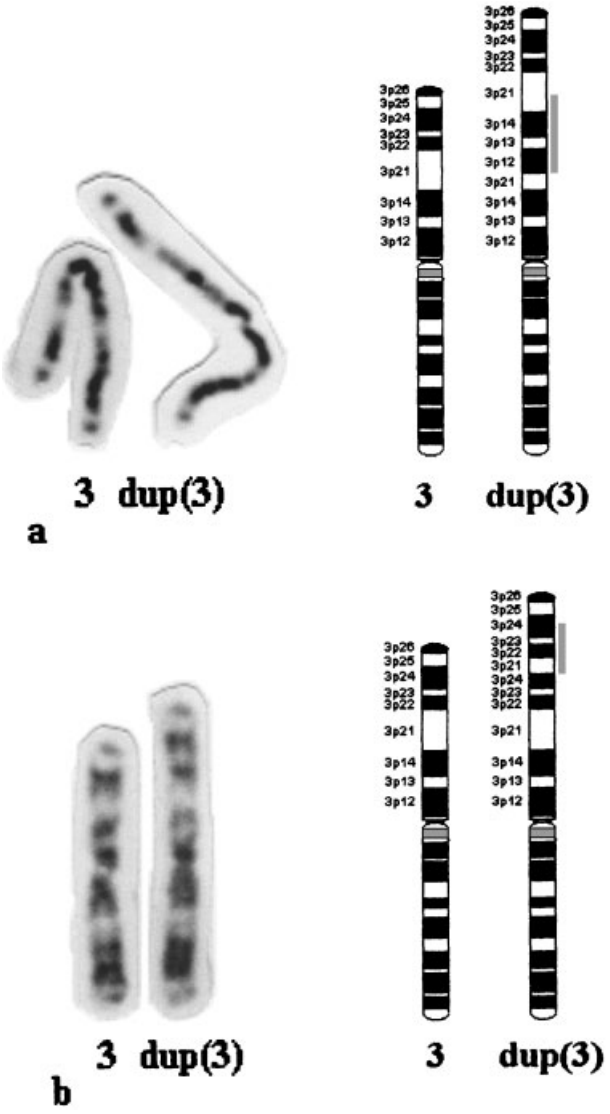

Fig. 2. Normal and duplicated chromosomes 3 after GTG-banding and ideograms depicting the duplications. Gray lines indicate the duplicated segments. **a:** Patient 1. **b:** Patient 2.

Patient 2

Cytogenetic analysis. A 3p21 → 3p24 tandem duplication was observed in 60 metaphases (Fig. 2b). The patient's mother had a normal karyotype and his father was not available. FISH of chromosome 3 short- and long-arm libraries confirmed the duplication of chromosome 3 short arm (Fig. 3f). The cosmids containing sequences of the genes *FHIT* (3p14.2) and *HSema IV* (3p21.31) were not duplicated. Near the proximal breakpoint, the YACs 712_a_7, 792_d_7 and 817_d_5 were duplicated, but YACs 730_c_5, 887_f_12, 796_d_2 and 758_g_3 were not. The YAC 749_a_7 was duplicated; however, its signals consistently had different intensities, the distal signal being always weaker,

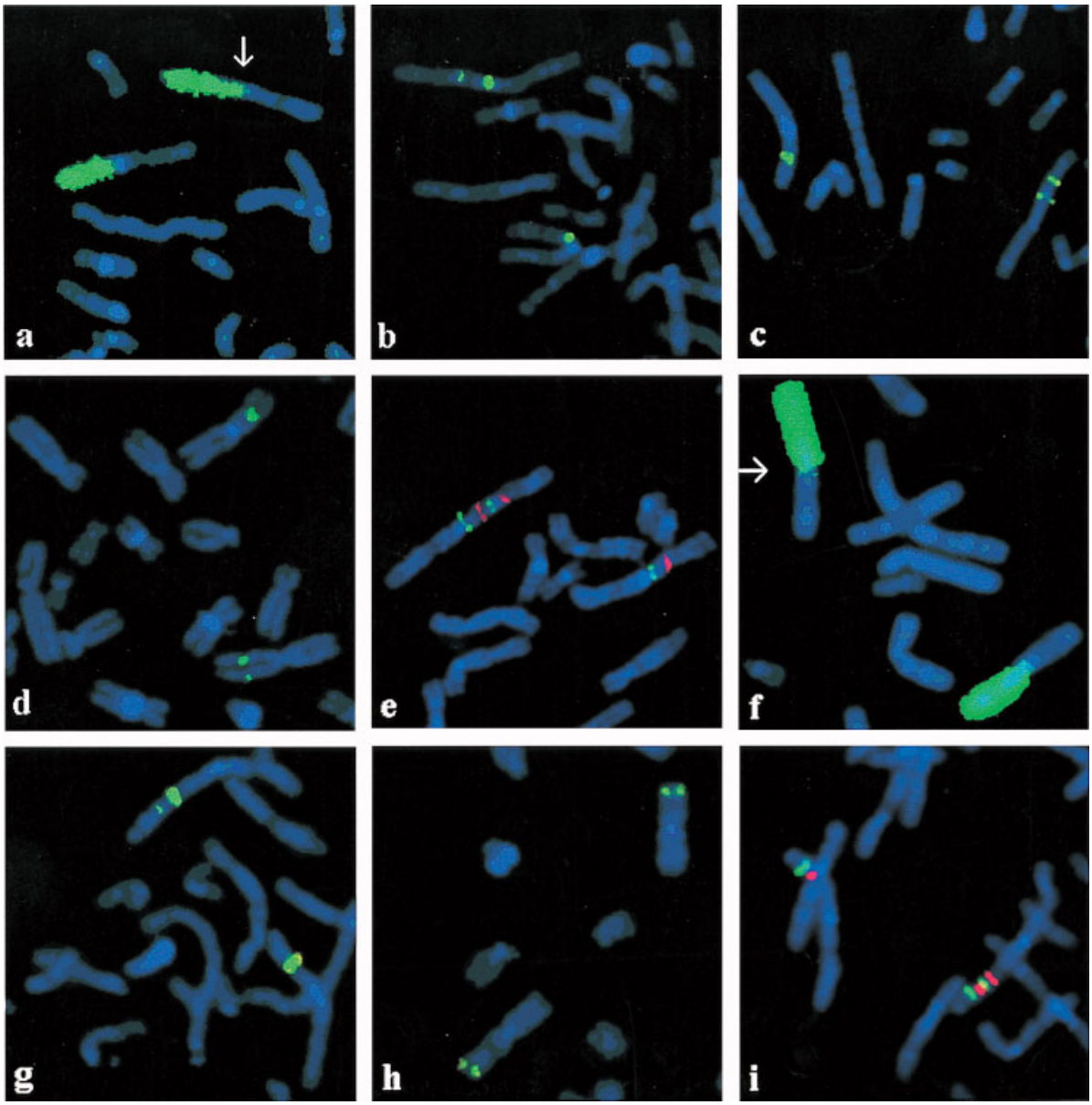

Fig. 3. Fluorescence in situ hybridization analysis: chromosome 3 short-arm library confirmed a 3p duplication in **(a)** Patient 1 and **(f)** Patient 2; arrows indicate the dup(3). Patient 1: **(b)** the partially duplicated YAC 961_h_3 contains the proximal breakpoint at p21.33; **(c)** the duplicated YAC 729_c_3 and **(d)** the nonduplicated YAC 806_h_2 delimit the interval of the distal breakpoint at 3p21.1; **(e)** dual-color hybridization of the YACs 796_c_4 (green signals) and 730_c_5 (red signals) evidences the direct duplication. Patient 2: **(g)** the partially duplicated YAC 749_a_7 contains the proximal breakpoint at 3p21.33; **(h)** the nonduplicated YAC 909_b_6 at 3p25, one of the boundaries of the distal breakpoint region; **(i)** dual-color hybridization of the YACs 932_b_6 (green signals) and 712_a_7 (red signals) evidences the direct duplication; YAC 932_b_6 at 3p24.3 is the most distal duplicated YAC.

thus indicating that this YAC was partially duplicated and spanned the proximal breakpoint (Fig. 3g). Supporting this interpretation, the flanking YACs 817_d_5 and 758_g_3 in WC 3.7 contig were duplicated and nonduplicated, respectively. The distal breakpoint was located between the YAC 909_b_6 (3p25.1), which was not duplicated (Fig 3h), and the duplicated YAC 932_b_6 (3p24.3). Dual-color FISH confirmed that the duplication was in tandem (Fig. 3i). Figure 4b summarizes FISH findings.

Microsatellite analysis. Twelve microsatellite loci were genotyped in the patient and his mother (Fig. 5b,d). In loci D3S1038, D3S2327, D3S2337, D3S1211, D3S1298, D3S3521, D3S3527, D3S3563, and D3S1296, the patient had two alleles and in loci D3S1110, D3S3598, and D3S1277, he was homozygous. Dosage coefficients were estimated for informative loci mapped to the duplicated segment as determined by FISH (D3S2327, D3S2337, D3S1211, D3S1298, D3S3521, and D3S3527). One of the alleles was more amplified than the other in loci

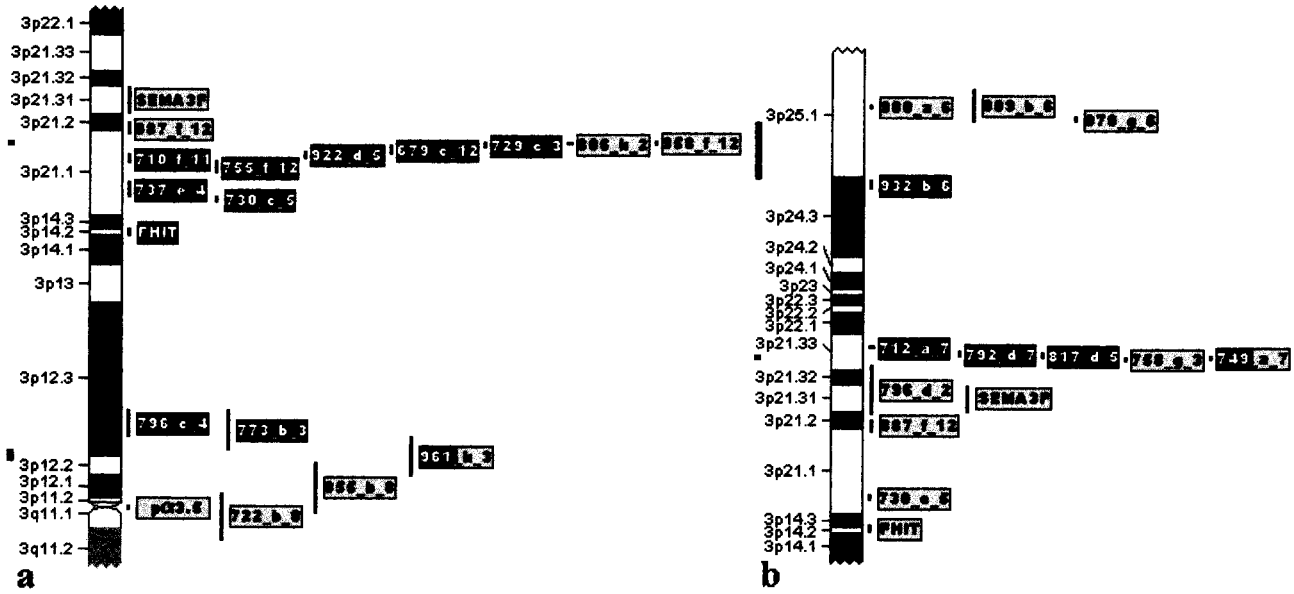

Fig. 4. Schematic representation of fluorescence in situ hybridization analysis in **(a)** Patient 1 and **(b)** Patient 2. Black boxes, duplicated probes; gray boxes, nonduplicated probes; black/gray boxes, partially duplicated probes. Black lines, the location of each probe (at right) and the breakpoint regions (at left) on chromosome 3 map.

D3S2327, D3S2337, D3S1211, D3S1298, D3S3521, and D3S3527. In loci D3S1298, D3S3521, and D3S3527, the duplicated alleles did not match with maternal alleles, pointing to a paternal duplication.

DISCUSSION

GTG-banding, FISH, and microsatellite analyses were associated in this study of two 3p duplications. FISH allowed the identification of the duplicated segments, and based on the location of these segments on the GDB maps, the position of breakpoints relative to chromosome bands could be more accurately mapped. Furthermore, YACs spanning breakpoints were identified, a first step in the study of the sequences involved in the rearrangements. In Patient 1, the YAC 961_h_3, mapped to the interface of 3p12.1 and 3p12.2, spanned the proximal breakpoint. The distal breakpoint was mapped between YACs 729_c_3 and 806_h_2, both at the distal end of 3p21.1. FISH and GTG-banding analyses agreed in the gross assignment of both breakpoints; however, the additional data provided by FISH allowed delimitation of the duplication as spanning the segment 3p12.2 to 3p21.1. Therefore, the patient's karyotype could be written as mos46,XY,dup(3)(p12.1or p12.2p21.1)/46,XY. In Patient 2, the proximal breakpoint was mapped to the YAC 749_a_7, at 3p21.33. The distal breakpoint was located between the YAC 932_b_6 at distal 3p24.3 and the YAC 909_b_6, mapped to 3p25.1. Since GTG-banding showed that 3p24.3 was partially duplicated, the breakpoint could be located at the distal end of 3p24.3. Therefore, the duplication spanned the segment 3p21.33 to 3p24.3, and the patient's karyotype was 46,XY,dup(3)(p21.33p24.3).

Microsatellite analysis enabled us to disclose the parental origin of the rearrangements, as well as their possible mechanisms of formation. Three alleles were never observed in our patients, and this required a quantitative analysis for the identification of the duplicated alleles. Since some alleles are amplified more efficiently than others, dosage coefficients were calculated by comparing the ratio between the smaller and the larger allele in the patients and their parents. These dosage coefficients are more precise when individuals bearing same-sized alleles are compared. This was the case when we compared allele intensities in loci D3S2336 and D3S1277 of Patient 1 and his father, as well as in the locus D3S1514 of this patient and his mother. Patient 2 and his mother had alleles of the same size in loci D3S1211, D3S2327 and D3S2337.

The presence of just two types of alleles on the duplicated segments of both patients indicated that the rearrangements occurred either postzygotically, or involved sister chromatids in meiosis. Allele dosage pointed to a paternal origin of both duplications. In Patient 1, the presence of a normal cell line makes a postzygotic origin of the duplication more likely. A meiotic rearrangement, however, remains a possibility, but requires additional events for the formation of the normal cell line, e.g., a duplicated chromosome present in all cells of a developing embryo can be lost and normality rescued by the duplication of the normal homologue, thus resulting in UPD for chromosome 3.

A rearrangement in the zygote between sister chromatids of the paternal chromosome would give rise to cells with a deletion and others carrying the tandem duplication. In the latter, paternal and maternal alleles would be present at the distal nonduplicated 3p, as in our patients. If the rearrangement occurred later in development, a normal cell line would also be present, as detected in Patient 1. The cell lines carrying the deletion might have been lost or restricted to tissues other than

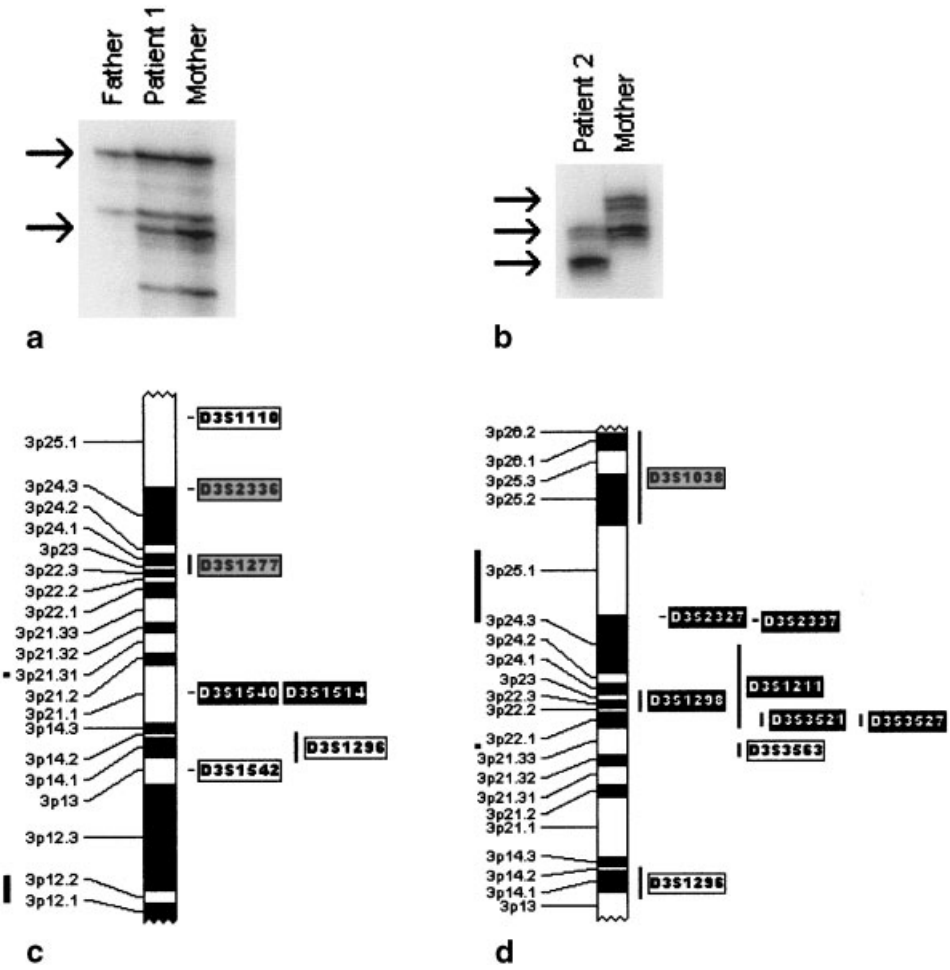

Fig. 5. Microsatellite analysis: **(a)** locus D3S1514 in Patient 1 and **(b)** locus D3S3521 in Patient 2, showing the duplication of paternal alleles (arrows point to the alleles). Schematic representation of microsatellite analysis in **(c)** Patient 1 and **(d)** Patient 2. Black boxes, duplicated loci; gray boxes, nonduplicated loci; white boxes, loci not studied by densitometry. Black lines, the position of each locus on chromosome 3 map (at right) and the breakpoint regions, as mapped by fluorescence in situ hybridization (at left).

blood. An exchange between homologous chromatids can be excluded, because in this case, the segregation of the duplicated chromatid with the paternal normal one would have resulted in a cell with a duplication of paternal loci and a deletion of maternal loci distally to the duplication.

The most important physical abnormalities of our Patient 1 were growth retardation and deformities in lower limbs. Pre- and postnatal growth retardation were present in 30% of the patients with chromosome 3 short-arm duplications reviewed by Conte et al. [1995], but lower limb deformities were not described. Among the 44 duplications reviewed, the one described by Kleckowska et al. [1984], which spanned the segment 3p14 → 3p22, partially overlapped the duplication present in our Patient 1 (3p12 → 3p21.1). This was also the case of the 3p11.1 → 3p14.2 duplication described by Watson et al. [1990]. Our patient, however, did not present a clinical picture in common with these patients.

Some of the patients reviewed by Conte et al. [1995] had duplications that overlapped, at least partially, the duplicated segment in our Patient 2 (3p21.33 → 3p24.3). The most similar rearrangement was the direct 3p21.3 → 3p25 duplication described by Zhang and Wang [1984]. Notwithstanding, this patient did not share a clinical phenotype with our Patient 2, whose main clinical features were macrosomy and macrocrania. Indeed, these features were not present in any of the patients with 3p duplication in the review of Conte et al. [1995].

Although the clinical delimitation of a "3p2 trisomy syndrome" has been attempted [Conte et al., 1995], different clinical pictures have been described in patients who carry duplications of the same chromosomal segment, e.g., the patients reported by Conte et al. [1995] and Frankova et al. [1991], both with 3p24.1 → 3pter duplication. In both cases, duplications originated from chromosomal translocations, and were associated with small deletions of other chromosomal segments. In fact, 39 of the 44 duplications reviewed originated from balanced rearrangements present in one of the parents, and the patients had deletions or duplications of other chromosomes that could contribute to the phenotypic variability. Alternatively, one may speculate that some

clinical manifestations might be influenced by the parental origin of the duplication. In this line of thinking, it is noteworthy that among the 3p21 → 3pter inherited duplications reviewed by Conte et al. [1995], six of the seven cases with a maternal origin had an early postnatal death, while only one of the five cases with a paternal origin died soon after birth. Certainly, the delineation of the phenotypic consequences of these chromosomal unbalances must go through the precise delimitation of duplicated/deleted segments and the identification of their parental origin.

ACKNOWLEDGMENTS

The authors thank Ms. Maria Raimunda L. S. Pinheiro for technical assistance.

REFERENCES

Christ LA, Crowe CA, Micale MA, Conroy JM, Schwartz S. 1999. Chromosome breakage hotspots and delineation of the critical region for the 9p-deletion syndrome. Am J Hum Genet 65:1387–1395.

Conte RA, Pitter JH, Verma RS. 1995. Molecular characterization of trisomic segment 3p24.1→3pter: a case with review of the literature. Clin Genet 48:49–53.

Floridia G, Piantanida M, Minelli A, Dellavecchia C, Bonaglia C, Rossi E, Gimelli G, Croci G, Franchi F, Gilgenkrantz S, Grammatico P, Dalpra L, Wood S, Danesino C, Zuffardi O. 1996. The same molecular mechanism at the maternal meiosis I produces mono- and dicentric 8p duplications. Am J Hum Genet 58:785–796.

Frankova YE, Holenova H, Braulke I. 1991. Partielle Trisome des kurzen Arms von Chromosom 3. Monatsschr Kinderheilkd 139:841–843.

Giglio S, Pirola B, Arrigo G, Dagrada P, Bardoni B, Bernardi F, Russo G, Argentiero L, Forabosco A, Carrozzo R, Zuffardi O. 2000. Opposite deletions/duplications of the X chromosome: two novel reciprocal rearrangements. Eur J Hum Genet 8:63–70.

Huang B, Crolla JA, Christian SL, Wolf-Ledbetter ME, Macha ME, Papenhausen PN, Ledbetter DH. 1997. Refined molecular characterization of the breakpoints in small inv dup(15) chromosomes. Hum Genet 99:11–17.

Katz SG, Schneider SS, Bartuski A, Trask BJ, Massa H, Overhauser J, Lalande M, Lansdorp PM, Silverman GA. 1999. An 18q-syndrome breakpoint resides between the duplicated serpins SCCA1 and SCCA2 and arises via a cryptic rearrangement with satellite III DNA. Hum Mol Genet 8:87–92.

Kleczkowska A, Fryns JP, Van den Berghe H. 1984. Partial trisomy of chromosome 3(p14-p22) due to maternal insertional translocation. Ann Genet 27:180–183.

Lupski JR. 1998. Genomic disorders: structural features of the genome can lead to DNA rearrangements and human disease traits. Trends Genet 14:417–422.

Page SL, Shin JC, Han JY, Choo KH, Shaffer LG. 1996. Breakpoint diversity illustrates distinct mechanisms for Robertsonian translocation formation. Hum Mol Genet 5:1279–1288.

Rosenberg C, Janson M, Nordenskjöld M, Borrensen AL, Vianna-Morgante AM. 1994. Intragenic organization of RB1 in a complex (4;13) rearrangement demonstrated by FISH. Cytogenet Cell Genet 65:268–271.

Rosenberg MJ, Vaske D, Killoran CE, Ning Y, Wargowski D, Hudgins L, Tifft CJ, Meck J, Blancato JK, Rosenbaum K, Pauli RM, Weber J, Biesecker LG. 2000. Detection of chromosomal aberrations by a whole-genome microsatellite screen. Am J Hum Genet 66: 419–427.

Sutton VR, Shaffer LG. 2000. Search for imprinted regions on chromosome 14: comparison of maternal and paternal UPD cases with cases of chromosome 14 deletion. Am J Hum Genet 93:381–387.

Wandstrat AE, Leana-Cox J, Jenkins L, Schwartz S. 1998. Molecular cytogenetic evidence for a common breakpoint in the largest inverted duplications of chromosome 15. Am J Hum Genet 62:925–936.

Watson MS, Dowton SB, Rohrbaugh J. 1990. Case of direct insertion within a chromosome 3 leading to a chromosome 3p duplication in an offspring. Am J Med Genet 36:172–174.

Waye JS, Willard HF. 1989. Chromosome specificity of satellite DNAs: short- and long-range organization of a diverged dimeric subset of human alpha satellite from chromosome 3. Chromosoma 97: 475–480.

Zhang SZ, Wang Q. 1984. Partial serial duplication of the short arm of chromosome 3. Chin Med J (Engl) 97:425–428.